Mechanical Properties and Deposition Mechanism of Hydrothermally Deposited Calcium Phosphate Coating

Sara Kaabi Falahieh Asl[a,b], Sandor Nemeth[b] , Ming Jen Tan[a]

[a] School of Mechanical & Aerospace Engineering, Nanyang Technological University, 639708 Singapore

[b] Singapore Institute of Manufacturing Technology, 638075 Singapore

Abstract

Biocompatible and bioresorbable magnesium and its alloys could be ideal alternatives for currently used implants (Ti, Co-Cr alloys) to avoid or minimise stress shielding effect which is the main drawback of currently used implants. However, the high corrosion rate of magnesium and its alloys limit their practical application. Thus, in this study, a hydrothermal coating process was developed to provide protective biocompatible and bioresorbable coatings. X-ray diffraction patterns indicated sharp and well-defined peaks corresponding to monetite at low deposition temperature and a mixture of monetite and tricalcium phosphate at higher deposition temperature. Scanning electron microscopy study of the morphology showed increasingly denser coating with higher deposition temperature. Coating adhesion properties were evaluated by pull-out test indicating cohesive failure at 5.2 to 5.8 MPa stress. The current coatings showed high hardness which decreased by increasing the deposition temperature. Raman spectroscopy studies showed that the coatings consisted of two distinct layers: tricalcium phosphate and monetite. Electrochemical impedance spectroscopy confirmed that the coatings provided varying levels of corrosion protection. The corrosion results showed that the size of capacitance loops and the absolute impedance value (|Z|) increased by increasing the deposition temperature and corresponding growth in coating thickness. It was found that coating was partially converted to hydroxyapatite after 28 days immersion in simulated body fluid, confirming the bioactivity of the coatings. The results confirmed that the obtained coatings could be a promising candidate for surface modification of Mg for implant application.

1. Introduction

Stainless steel, titanium and cobalt-based alloys, as well as various ceramic materials are commonly used for implants to support fractured human bones. However, due to mismatches in mechanical properties between the implants and bones, stress shielding effect is present, and release of poisonous ions by corrosion or mechanical wear is a danger. Additionally, a second surgery is frequently needed to remove the implant after healing is complete [1-4]. Metallic biodegradable implant material is desirable in cases when no further support is needed after bone healing. Recently, magnesium alloys have attracted significant interest as biodegradable implant materials due to their excellent properties. Magnesium plays a major part in metabolism and can dissolve completely in body environment. Therefore, the need for a second operation after bone healing to remove the implant is eliminated. Since the mechanical properties of magnesium are closer to that of bone than conventional implant materials the stress shielding effect could be avoided or minimised as well [5-7].

The ions released due to the corrosion of magnesium in the body can be absorbed in the tissues or eliminated over time. The dissolution of magnesium implants also decreases the chance of an immune response [4-9]. The decrease in immune response is due to the continuous formation of fresh interface between the living tissue and implant as the surface dissolves, thus reducing the chance of sheltering bacteria and other microorganisms at the non-living material surface where the immune system may have limited access. However, the high degradation rate of magnesium alloys is the major reason that limits or even prevents their large-scale use, resulting in rather rapid loss of mechanical integrity in human body environments [2, 7]. Hence, enhancing the corrosion resistance of magnesium alloys and preventing the quick loss of their strength is an outstanding challenge that, if

addressed, can lead to more widespread biomedical applications and possibly other industrial uses [8, 10]. In case of biomedical applications, a relatively modest extension of implant lifetime of two to ten-fold improvement is sufficient. When using temporary implants, full healing usually takes place in less than a year. Thus, extending the lifetime of the implant for up to one year in the body is adequate.

During the last decades of research, a number of methods were developed for the deposition of HA (hydroxyapatite) coatings on metallic implants, including: electrodeposition [11, 12], sol-gel coating [13], and biomimetic methods [14]. These coatings could potentially offer protection to the Mg alloy substrate; however, in the case of biomimetic method coatings are extremely permeable, and exhibit many cracks [15] or in the electrodeposition method, the release of hydrogen bubble on the Mg surface creates imperfections in the coating resulting in poorly adherent and non-uniform layer. The hydrogen bubbles adhere to the surface and impede the nucleation and deposition of coating [12, 16]. Therefore, there is a clear need to deposit high performance coatings which pass the entire requirement such as corrosion resistance, biocompatibility, bioactivity and enough adhesion strength for the orthopaedic application. Therefore, a new hydrothermal method is presented in this work for producing dense and adherent coatings over a large surface area suitable even for irregular geometry. Deposition of Ca-P ceramic coating on the surface of AZ31 alloy, the analysis of the coating properties, and its corrosion protection is discussed in the present paper.

2. METHODOLOGY

2.1 Experimental Procedures

Analytical grade $Ca(NO_3)_2$ (99.98% purity) and $NH_4H_2PO_4$ (98% purity) were obtained from Alfa Aesar. AZ31 magnesium alloy was used as substrate for the coating process. Disks were prepared with 25 mm diameter and 2 mm thickness using commercial AZ31 rod. Prior to coating process, AZ31 substrate was abraded with up to 2400 grit abrasive paper, and then ultrasonically cleaned in acetone for 20 minutes. In order to deposit Ca-P coating on the Mg substrate; hydrothermal process was used. A solution of $Ca(NO_3)_2$ (0.1M) and $NH_4H_2PO_4$ (0.06 M) was prepared for the process. The pH of solution was adjusted to 3.9-4.0 by using ammonia. The AZ31 samples and deposition solution were placed in a stainless steel autoclave with polytetrafluoroethylene lining and heated in an electric oven at different temperatures (100 ºC, 130 ºC, 160 ºC and 190 ºC) for 3 hours. The samples were named as HE100 ºC-3hr, HE130 ºC-3hr, HE160 ºC-3hr and HE190 ºC-3hr according to the respective deposition temperature and time.

Note: Magnesium may generate hydrogen in aqueous environment that could increase the pressure significantly and allowance must be made for such potential pressure rise to safely conduct the hydrothermal process.

2.2 Coating Characterization

The surface phase of the coated samples was characterized by X-ray diffractometer (XRD, Panalytical Empyrean, DY2t), using Cu-Kα1 radiation (wavelength λ= 1.5406Å). The surface morphology and the chemical composition were analyzed using scanning electron microscope (JEOL JSM 5600 SEM) with an EDS (INCA system, Oxford Instruments, UK).

The Raman scattering measurements were performed using a Raman microprobe instrument (RENISHAW-in Via Raman Microscope). Raman spectra were collected over the frequency range 100-1500 cm^{-1}, with a spectral resolution of 1 cm^{-1}. The 488 nm line of an Ar^+ laser was used as excitation source. Raman measurements were done through the coating cross section. For this purpose samples were cold mounted and after cutting the samples the cross section were prepared with up to 4000 grit abrasive paper, and mechanically polished up to 0.5 micron using alumina slurry.

In order to investigate the corrosion behavior of coatings, electrochemical impedance spectroscopy (EIS) test was performed in simulated body fluid (SBF) [18] solution at pH 7.2 using a Solarton potentiostat (Model SI 1260). The EIS tests were conducted at the open circuit potential (OCP) in the frequency range of 100 kHz to 10 mHz, using 10 mV amplitude of signal's perturbation

The immersion tests were conducted in the SBF standard solution for up to 28 days in order to assess the early corrosion performance of the coated and uncoated substrate. Each sample with an exposure area of 4.9 cm^2 was immersed in 50 ml of the SBF solution at 37 ºC.

For characterizing the mechanical response, nano-indentation experiments were conducted using a Berkovich diamond indenter (Hysitron). A maximum load of up to 4000 µN was used.

Adhesion strength between coating layer and AZ31 substrate was evaluated based on ISO 13779-4. Pull-out test was carried out by using Instron testing machine at a cross head speed of 1 mm/min

3. RESULTS & DISCUSSION

3.1. *Surface characterization and deposition mechanism*

By increasing the temperature, calcium/phosphate salt solubility decreased and consequently the solution became supersaturated resulting in Ca-P mineral deposition on the surface of Mg substrate. At pH below 5, biocompatible and bioresorptive monetite and calcium pyrophosphate are the most stable phosphate phases. However, the presence of Mg ions can stabilize the tricalcium phosphate phase. The stabilizing effect of Mg is attributable to the markedly smaller ionic radius of Mg^{2+} (0.65 Å) compared to Ca^{2+} (0.99 Å) [17]. The XRD analysis indeed showed that coated materials obtained from the hydrothermal process were a mixture of monetite ($CaHPO_4$), tricalcium phosphate, and calcium pyrophosphate ($Ca_2P_2O_7$) as shown in Fig.1.

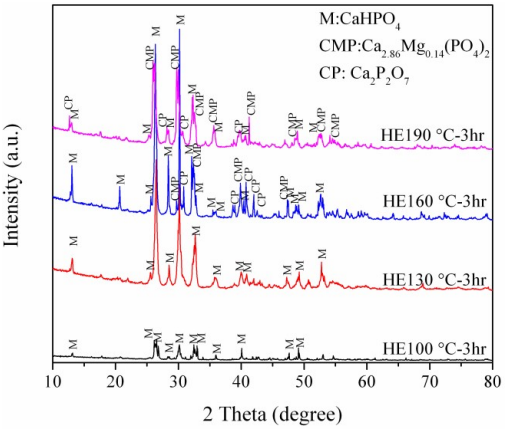

Fig.1. XRD pattern of coatings on AZ31 at different deposition temperatures

The morphology of Ca-P coating obtained from the hydrothermal process is shown in Fig.2. The coating morphologies are compact, pore free, and clearly show triclinic structure. The coated sample at 100 ºC displayed a plate like morphology. By increasing the deposition temperature, the gap size between crystals decreased and the coating became denser. Additionally, the amount of deposited Ca-P and the size of crystals increased significantly. The solubility of Ca-P decreases with increasing the temperature; consequently, a higher amount of Ca-P is deposited on the substrate. Moreover, diffusion rate increases by increasing the deposition temperature; hence, the reactants move to the substrate more easily. During the initial phase of the hydrothermal process, the deposition solution (pH: 3.9-4.0) etches the Mg substrate and forms a rough metal surface with pits. The etched pits in the surface of Mg substrate may act as nucleation sites for Ca-P deposition and growth [18].

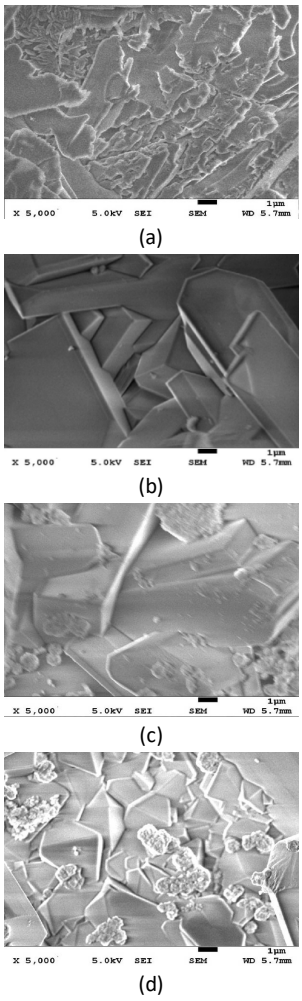

Fig.2. SEM micrograph of coated AZ31 (a) 100 ºC, (b) 130 ºC, (c) 160 ºC and (d) 190 ºC. In all cases, the deposition time was 3 hours

In order to understand the deposition mechanism, Raman spectroscopy mapping analysis was done through the coatings cross section as shown in Fig.3 for the sample coated at 160 ºC. Based on the cross section study, coating is composed of two different layers, which can be distinguished through their main corresponding Raman peaks. The layer adjacent to the magnesium substrate contains predominantly tricalcium phosphate [$Ca_3(PO_4)_2$] or to be more precise whitlockite phase with the main Raman peak at 970 cm^{-1}. This layer started to deposit on the AZ31 substrate at the early stages of coating formation. This was followed by the deposition of a second layer mainly consisting of monetite phase with the main Raman peaks at 987 cm^{-1}.

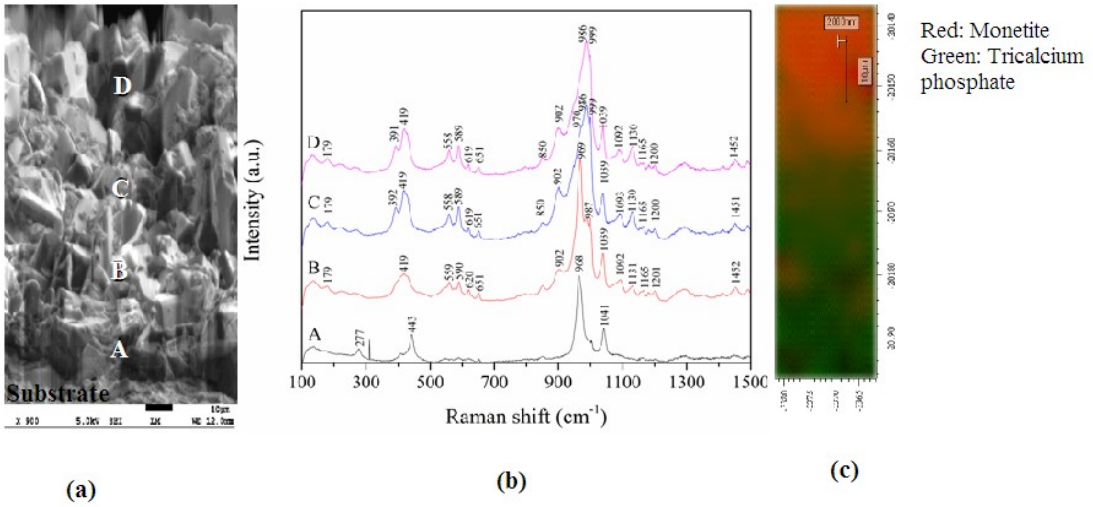

Fig.3.Raman spectroscopy characterisation of coatings: a) SEM cross section, b) Raman pattern through the cross section, c) Raman map review through the cross section

Mg rapidly corrodes at low pH. As a result of Mg corrosion, the local pH close to the substrate surface increases. The rise in the local pH can exceed the pH stability range of tricalcium phosphate which results in the solution's super saturation and promotes the deposition of tricalcium phosphate crystals as a first deposited layer. Moreover, the presence of Mg ions (released through substrate corrosion) can stabilize the tricalcium phosphate phase as well due to the markedly smaller ionic radius of Mg^{2+} (0.65 Å) compared to Ca^{2+} (0.99 Å) [19-21]. The EDS analysis through the cross section of coated sample on Mg substrate that was formed at 160 °C confirmed that Mg ions contributed to the coating layer with high abundance near the substrate. However, the Mg concentration diminished as the distance from the substrate increased, as shown in Fig.4.

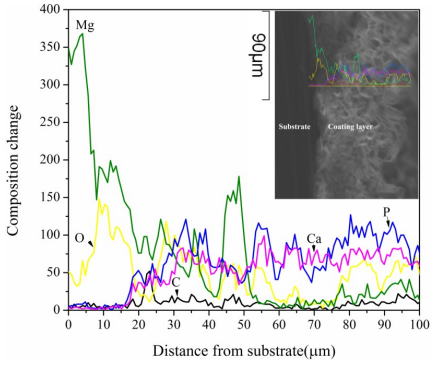

Fig.4. EDS analysis through the coating cross section for coated sample at 160 °C

Initial deposition of tricalcium phosphate on the Mg substrate can isolate the metal from solution attack. Thus, after a thin coating layer is formed, the effect of magnesium corrosion on the local pH of the solution is diminished. Further Ca-P deposition is influenced only by the solution pH (pH is 3.9 to 4.0) that is conducive for monetite phase formation on top of the tricalcium phosphate layer. Therefore, the coating was composed of two different crystalline layers (tricalcium phosphate and monetite).

3.2. Mechanical properties and adhesion behaviour of coatings

Coating adhesion was evaluated by means of pull-off test. The stress-displacement curves obtained from pull-out adhesion tests and coating morphology after adhesion test are shown in Fig.5 and the results are summarized in Table.1. For the samples prepared at 100 ºC, 130 ºC and 160 ºC, the coatings failed by cohesive failure at around 5.2-5.8 MPa. At preparation temperature of 190 ºC, the coated sample failed at around 3.1 MPa, probably due to the increase in coating thickness and increasing the residual stress in the coating layer. The SEM micrograph of coating after pull of test clearly showed that coating still remained on the substrate.

Mechanical properties of coatings were measured by means of nanoindentation. Fig.6. show a comparison between mechanical properties of coatings. Ca-P inorganic coating shows high hardness and Young's modulus. By increasing the deposition temperature the hardness and Young's modulus of coatings decreased, probably due to the incorporation of Mg ions into the coating structure.

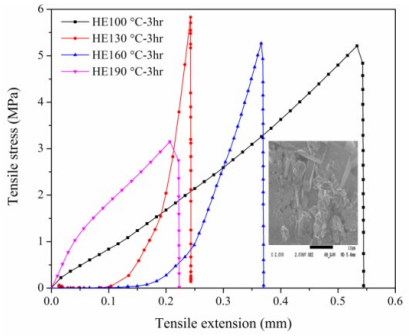

Fig.5. Coatings adhesion to the substrate

Table1. Coatings adhesion strength

Temperature(˚C)	Hardness(GPa)	Young modulus(GPa)
100	6.1	109.2
130	6.0	105.2
160	5.8	98.6
190	2.5	55.2

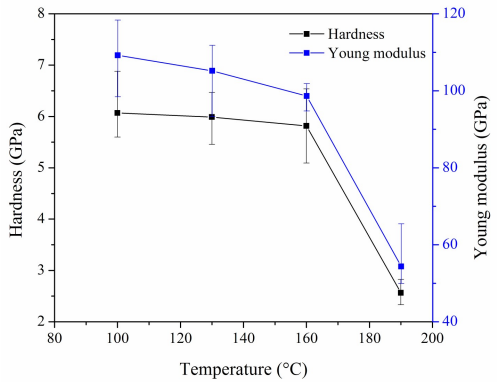

Fig.6. Comparison between Young moduli and hardness of coatings

3.3 Corrosion performance and degradation behaviour of coatings

EIS measurements were analyzed by means of Nyquist impedance spectroscopy for the bare and coated samples as given in Fig.7. It was clearly observed that the Nyquist graph for bare sample composed of two capacitive semi-circuits at medium and low frequency, followed by an inductive loop at low frequency region. The time constant at medium frequency can be attributed to the partially protective oxide layer and semi-circle at low frequency might be related to the charge transfer resistance (Rct) and double layer capacitance (Cdl) at the surface of substrate [22]. The appearance of inductive loop at low frequency is probably due to film weakening and pit incubation. Coated samples at 100 ºC, 130 ºC and 160 ºC only showed a capacitance loop at medium frequency. The capacitive loop at medium frequency might be attributed to the coating layer polarization resistance (Rp).

The calculated capacitances for these time constants were in the range of 4-12 µF. Since the double layer capacitance is normally between 20-50 µF [23], the appearance of this semi-circle is related to coating layer resistance. The size of capacitance loops was increased by increasing the deposition temperature. This is in parallel to the increase in charge transfer and polarization resistance which is a criterion for corrosion resistance enhancement [24].

The coated sample at 190 ºC showed a different behavior. For the coated samples at 190 ºC, the Nyquist graph was composed of two capacitive loops at high and medium frequency. The high frequency time constant can be related to coating layer resistance and the presence of capacitive loop at medium frequency range can be related to the new surface formation at the electrode surface as a result of partial delamination of top surface of coating [25].

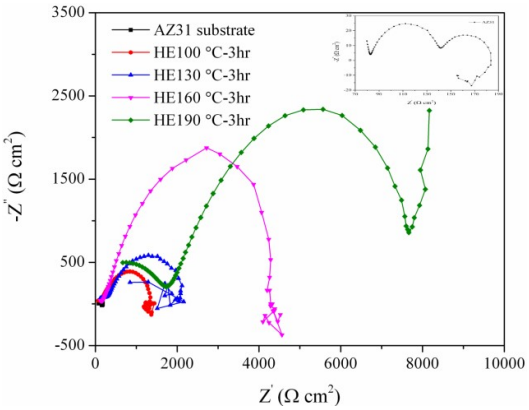

Fig.7. Nyquist of uncoated and coated samples in SBF solution

The degradation rate of Mg and its alloys in the initial stages of implantation would play a significant role in the new formed tissue response. If the early degradation rate of Mg-based implants is too rapid, pre-implantation and osteolysis reaction would take place, consequently, negatively affecting bone tissue regeneration and healing. Fig.8 shows the mass loss for uncoated AZ31 substrate and Ca-P coated samples. The mass loss of samples was measured during the immersion period. The total mass lost from the uncoated AZ31

was approximately 38.7 mg/cm^2 after 28 days immersion in SBF solution, while for coated samples the figures were much smaller. For the coated sample at 160 ºC the total mass loss was 14.3 mg/cm^2 after 28 days. In the case of coated samples at 130 ºC and 100 ºC the mass loss after 28 days was 21.8 and 27.63 mg/cm^2.

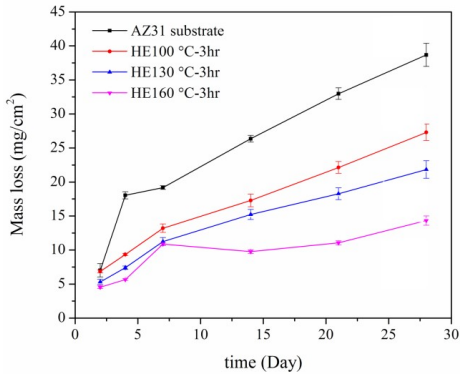

Fig.8.Mass loss for uncoated AZ31 and coated samples as a function of immersion time

Photographs of tested samples after 28 days immersion in SBF are shown in Fig.9. As it can be seen from the photographs, the uncoated Mg substrate undergoes severe and non-uniform corrosion after 28 days immersion in SBF solution. As immersion time increased, the pits on the surface of Mg became wider and started to penetrate through the substrate thickness (the photographs of other immersion times are not shown here). In some part of substrate pits propagated through the whole 2 mm substrate thickness leading to premature loss of mechanical integrity. On the other hand, the coated samples at 130 ºC and 160 ºC depositions displayed intact coating and no obvious pits were observed on the coating surface. Since the $Mg(OH)_2$ layer is not protective and can transform into soluble $MgCl_2$, the breakdown of $Mg(OH)_2$ layer can provide more active sites which accelerates the corrosion of substrate. Moreover, the difference in electrochemical activities of different phases in Mg results in the formation of microcells and consequently galvanic corrosion can happen after dissolution of protective layers resulting in the formation of a non-uniform corrosion process [26].

SEM images of the bare and coated samples after 28 days immersion test are shown in Fig.10. From the SEM micrograph it is clear that surface of Mg substrate undergoes severe corrosion and shows a rough appearance. However, in the case of coated sample at 160 ºC, the coating layer still remained on the surface of substrate but Ca-P crystals started to dissolve as some pits appear on the surface of the Ca-P crystals. Formation of pits on the surface of Ca-P crystals might be attributed to the dissolution of monetite. Monetite is a stable phase below pH value around 5. Since the pH was around 7.2-7.4 in the SBF solution, this higher pH could break down the thermodynamic equilibrium at the interface of monetite and solution and results in dissolution of monetite phase according to Eq.1 [27].

$$CaHPO_4 \rightarrow Ca^{2+} + HPO_4^{2-} \quad (1)$$

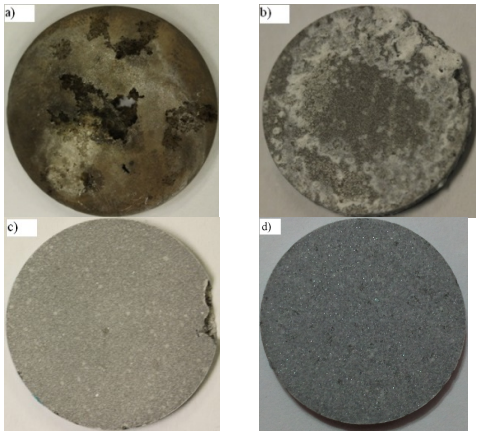

Fig.9.Photographs of tested samples after 28 days immersion: a)AZ31 substrate, b) HE100 °C-3hr, c) HE130 °C-3hr, d) HE160 °C-3hr

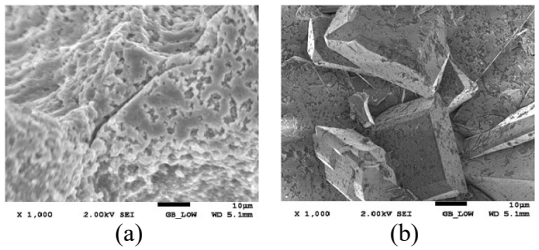

(a) (b)

Fig.10.SEM micrograph of: a) AZ31 substrate, b) HE160 °C-3hrafter 28 days immersion in SBF solution

Conclusion

Compact and pore free Ca–P coatings were successfully deposited on the Mg substrate by the hydrothermal method at different temperatures. The obtained coatings were mainly a mixture of bioactive and resorbable monetite and tricalcium phosphate phases, as confirmed by means of XRD technique.

Deposition of Ca-P coatings were affected by corrosion of substrate in the first step of deposition process inducing pH change in the vicinity of the metal and promoting Ca-P precipitation on the surface. The coatings were composed of two different layers. The formation of first deposited layer (tricalcium phosphate) is promoted by increased local pH by the interface reaction while

the second layer (monetite) is deposited at bulk solution pH.

Significant corrosion protection was achieved by the hydrothermal coating layer as indicated by the dissolution behavior of the Mg substrate and the Ca–P coated sample in the immersion test. The mass loss for the coated samples after 28 days was only one-third of the uncoated samples.

EIS results showed that the size of capacitance loops increased after applying the coating layers on Mg substrate and the capacitance loop's size was increased by increasing the deposition temperature. This is in parallel to the increase in charge transfer and polarization resistance.

Overall, the reported coatings have several beneficial functions that can accelerate the more widespread application of magnesium as an implant material. Further research using in-vitro and in-vivo techniques would be necessary to fully characterise and qualify the reported coatings for magnesium implants along with optimizing their mechanical properties in order to be adjustable to that of human bone. These studies will be the subject of future reports.

REFERENCES

1. Witte, F., *The history of biodegradable magnesium implants: a review.* Acta Biomater, 2010. **6**(5): p. 1680-92.

2. Witte, F., et al., *Biodegradable magnesium-hydroxyapatite metal matrix composites.* Biomaterials, 2007. **28**(13): p. 2163-74.

3. Witte, F., et al., *Degradable biomaterials based on magnesium corrosion.* Current Opinion in Solid State and Materials Science, 2008. **12**(5-6): p. 63-72.

4. Zeng, R., et al., *Progress and Challenge for Magnesium Alloys as Biomaterials.* Advanced Engineering Materials, 2008. **10**(8): p. B3-B14.

5. Hornberger, H., S. Virtanen, and A.R. Boccaccini, *Biomedical coatings on magnesium alloys - a review.* Acta Biomater, 2012. **8**(7): p. 2442-55.

6. Salahshoor, M. and Y. Guo, *Biodegradable Orthopedic Magnesium-Calcium (MgCa) Alloys, Processing, and Corrosion Performance.* Materials, 2012. **5**(12): p. 135-155.

7. Salunke, P., V. Shanov, and F. Witte, *High purity biodegradable magnesium coating for implant application.* Materials Science and Engineering: B, 2011. **176**(20): p. 1711-1717.

8. Song, G. and S. Song, *A Possible Biodegradable Magnesium Implant Material.* Advanced Engineering Materials, 2007. **9**(4): p. 298-302.

9. Xu, L. and A. Yamamoto, *Characteristics and cytocompatibility of biodegradable polymer film on magnesium by spin coating.* Colloids Surf B Biointerfaces, 2012. **93**: p. 67-74.

10. Song, G., *Control of biodegradation of biocompatable magnesium alloys.* Corrosion Science, 2007. **49**(4): p. 1696-1701.

11. Lin, D.-Y. and X.-X. Wang, *Preparation of hydroxyapatite coating on smooth implant surface by electrodeposition.* Ceramics International, 2011. **37**(1): p. 403-406.

12. Song, Y.W., D.Y. Shan, and E.H. Han, *Electrodeposition of hydroxyapatite coating on AZ91D magnesium alloy for biomaterial application.* Materials Letters, 2008. **62**(17–18): p. 3276-3279.

13. Kim, H.W., et al., *Sol-gel derived fluor-hydroxyapatite biocoatings on zirconia substrate.* Biomaterials, 2004. **25**(15): p. 2919-26.

14. Keim, S., et al., *Control of magnesium corrosion and biocompatibility with biomimetic coatings.* J Biomed Mater Res B Appl Biomater, 2011. **96**(1): p. 84-90.

15. Shadanbaz, S. and G.J. Dias, *Calcium phosphate coatings on magnesium alloys for biomedical applications: A review.* Acta Biomater., 2012. **8**(1): p. 20-30.

16. Hornberger, H., S. Virtanen, and A.R. Boccaccini, *Biomedical coatings on magnesium alloys – A review.* Acta Biomater., 2012. **8**(7): p. 2442-2455.

17. Salimi, M.H., J.C. Heughebaert, and G.H. Nancollas, *Crystal growth of calcium phosphates in the presence of magnesium ions.* Langmuir, 1985. **1**(1): p. 119-122.

18. Liu, D., K. Savino, and M.Z. Yates, *Coating of hydroxyapatite films on metal substrates by seeded hydrothermal deposition.* Surface and Coatings

Technology, 2011. **205**(16): p. 3975-3986.

19. *Boanini, E., M. Gazzano, and A. Bigi, Ionic substitutions in calcium phosphates synthesized at low temperature. Acta Biomater, 2010. 6(6): p. 1882-94.*

20. Lagier, R. and C.A. Baud, Magnesium whitlockite, a calcium phosphate crystal of special interest in pathology. Pathol Res Pract, 2003. 199(5): p. 329-35.

21. Morikawa, H., et al., Effects of magnesium for calcium substitution in P2O5–CaO–TiO2 glasses. Journal of Non-Crystalline Solids, 2013. 380: p. 53-59.

22. J. Fan, X. Qiu, X. Niu, Z. Tian, W. Sun, X. Liu, Y. Li, W. Li, J. Meng, Microstructure, mechanical properties, in vitro degradation and cytotoxicity evaluations of Mg-1.5Y-1.2Zn-0.44Zr alloys for biodegradable metallic implants, Mater. Sci. Eng., C 33 (2013) 2345.

23. W.A. Badawy, N.H. Hilal, M. El-Rabiee, H. Nady, Electrochemical behavior of Mg and some Mg alloys in aqueous solutions of different pH, Electrochim. Acta 55 (2010) 1880.

24. S. Creager, 3 - Solvents and Supporting Electrolytes, in: G.Z. Cynthia (Ed.) Handbook of Electrochemistry, Elsevier, Amsterdam, 2007, pp. 57-IV.

25. Z. Yao, Z. Jiang, F. Wang, Study on corrosion resistance and roughness of micro-plasma oxidation ceramic coatings on Ti alloy by EIS technique, Electrochim. Acta 52 (2007) 4539.

26. G. Ballerini, U. Bardi, R. Bignucolo, G. Ceraolo,About some corrosion mechanisms of AZ91D magnesium alloy, Corros. Sci 47 (2005) 2173.

27. Y. Wang, C.S. Lim, C.V. Lim, M.S. Yong, E.K. Teo, L.N. Moh, In vitro degradation behavior of M1A magnesium alloy in protein-containing simulated body fluid, Mater. Sci. Eng., C 31 (2011) 579